LARGE-EDDY SIMULATION OF INDOOR DISPERSION OF EXPIRATORY AEROSOL

Takamasa Hasama[1]
[1]Technica Research Institute, Kajima Corporation, Tokyo, Japan,
takamasa@kajima.com

ABSTRACT

This paper presents the decay characteristics of expiratory aerosol in indoor large-eddy simulations (LES) coupling with Lagrangian particle tracking in terms of preventing ability evaluation to the pathogen infection in a typical indoor environment. A Lagrangian method, which is able to simulate water droplet behaviour with seven particle diameters, was adopted simultaneously. Five enclosed-room cases with different diffuser-induced airflow patterns were investigated, all under the same air change per hour (ACH) condition. In particular, we focus on the decay characteristics of a typical office environment, unlike hospital isolation rooms to control airborne spores. The results show that for particles about 10.0 μm in diameter, which closely approximates the mean diameter of expiratory aerosol generated when coughing or speaking, the decay characteristics of the floor-supplied displacement type proved most efficient, followed by the ceiling-mounted breeze-line diffuser, third is the floor-mounted diffuser, fourth is the ceiling-mounted square diffuser, and least effective was the ceiling-mounted four-way cassette-type HVAC unit, under the same ACH.

INTRODUCTION

We spend over 85 percent of the time in confined microenvironments, i.e. transport, workplace, and residence (Klepesis et al., 2002). The apparent importance of controlling airborne transmission of infectious agents in indoor environments is well recognized. Today, controlling and reducing person-to-person airborne transmission of highly contagious diseases is a growing concern. The severe acute respiratory syndrome (SARS) outbreak in 2003 and the so-called swine flu (H1N1) pandemic in 2009 stimulated a series of engineering investigations into the transmission mechanisms for airborne infectious diseases within buildings. The recent increased interest in studying engineering control methods for airborne diseases is also associated with rapid social and environmental changes, such as urbanization, high density living, international air travel, and climate change, which have increased the risk of the emergence, re-emergence, and spread of different infectious diseases, especially airborne diseases (Weiss et, al., 2004). In general, aerosol dynamics differ from gaseous pollutants due to the effects of gravity, inertia and deposition on solid surfaces. Proper understanding of aerosol transport is required to improve exposure assessment tools and models and adopt better ventilation strategies that can substantially reduce indoor particle concentrations and improve indoor air quality. When coughing, sneezing, talking or breathing, people inherently generate particles of different sizes and air jets with different initial characteristics. In their latest findings, Chao et al. summarized the scarce data on the particle size distribution of expiratory aerosols (Chao et al., 2009). The airflow pattern is the most significant parameter influencing droplet transport in indoor environments (e.g. Chao et al., 2006). The choice of ventilation scheme controls the global airflow pattern and thus the ultimate distribution of pollutants. A recent study has shown that the unidirectional upward ventilation system is more efficient in removing small droplets, while the single floor system is more efficient in removing large droplets (Chao et al., 2006; Wan et al., 2007). These studies showed that in order to design an effective ventilation system, it is crucial to have a reliable tool that is able to predict airflow patterns and particle distribution and dispersion indoors. This can be achieved through the use of computational fluid dynamics (CFD), which has the capacity to provide microscopic information on the indoor air environment. In terms of CFD methods, typically the Reynolds-averaged Navier-Stokes (RANS) simulation is used to predict indoor airflow patterns. However, most RANS-based CFD methods have certain drawbacks, especially when predicting unsteady phenomena and complex flow geometry. On the other hand, large-eddy simulation (LES) is recognised as a powerful tool for satisfying the constant desire for more accurate predictions. LES directly resolves the transient behaviour of large-scale turbulent motion, which tends to have the greatest influence on turbulent transport, yet fewer adjustable constants are required (Zhang et al., 2000). LES resolves time-dependant turbulent flows with three-dimensional turbulent phenomena. Thus, LES can account for the history and transport effects of turbulence on aerosol dispersion and deposition. Generally speaking, LES requires far more computing power, and by extension cost, than RANS.

However, developments in computing speed and falling prices now enable LES computations to be carried out using current computer resources, so many recent tasks have concerned a number of indoor airflow problems (e.g. Berrouk et al., 2009).

In this paper, in terms of evaluating the ability to prevent pathogen infections in typical indoor environments, the decay characteristics of expiratory aerosol in indoor environments was investigated using LES coupling with Lagrangian particle tracking. A Lagrangian method, which is able to simulate water droplet behaviour with seven particle diameters, was adopted simultaneously. This investigation focuses on the decay characteristics of typical office environments, unlike hospital isolation rooms for airborne spores. Indeed, it is important to introduce the latest airflow technology (e.g. Bolashikov et al., 2009) so as to control and reduce person-to-person airborne transmission. However, it is likely that heating, ventilating and air-conditioning (HVAC) systems will remain the norm in most large buildings, especially offices. Therefore, we consider it more practical to combine the existing HVAC systems with removal or eradication approaches such as ultraviolet germicidal irradiation (UVGI) systems (e.g. Sung et al., 2010). The goal of this study was to create an airflow design method that enabled the risk of airborne pathogen infection to be reduced by combining a conventional HVAC system with an additional removal system, such as UVGI. As a first step, it is necessary to clarify the behaviour of airborne pathogens, i.e. dispersion of coughed spit droplets in typical indoor environment airflow patterns induced by the most common air inlet-outlet layouts. Five enclosed-room cases, with different diffuser-induced airflow patterns were investigated; namely four-way cassette-type diffuser, square-type diffuser, breeze-line-type diffuser, floor-supplied diffuser and full-floor supplied displacement type, all under the same air change per hour (ACH) condition.

CALCULATION CONDITIONS

Calculation case

Figure 1 shows the calculation environment and initial particle position. In this paper, when investigating the indoor decay process of spit droplets in locations where multiple people congregate, it is difficult to specify the position where the expiratory aerosol is generated. Therefore, particles are placed at the respiratory height position in a sedentary state (h=1~1.2 m, shown as a particle cloud position in Fig. 1) in advance for typical indoor airflow environments using a common air inlet-outlet layout. The calculation cases are shown in Table 1, while the calculation space configuration of each case is shown in Fig. 2. Each case has the same dimensions and ACH (=16, equivalent to 1,769 m^3/h) condition. The nominal time constant is 225 s. The room dimensions are 6.4 m × 6.4 m × 2.7 m (L×W×H), which assumes the minimum configuration of a typical office layout module. Five enclosed-room cases, with different diffuser-induced airflow patterns are considered; (1) Case 4WC: This case replicates a standard four-way cassette type HVAC unit, and has 16 inlets and 4 outlets in total, all set in the ceiling; (2) Case BLD: This case replicates the breeze-line-type diffuser unit, and has 4 inlets and 2 outlets in total, all set in the ceiling; (3) Case SD: This case replicates the square-type diffuser unit, which has 6 inlets and 2 outlets in total, both set in the ceiling; (4) Case FD: This case replicates the floor-supplied diffuser unit, which has 16 inlets set into the floor and 2 outlets in the ceiling; and (5) Case FSD: This case replicates a full-floor supplied displacement type. Inlet air is supplied across the entire floor area, and 2 outlets are set in the ceiling. In each case, the turning of diffusion characteristics that calibrate the modelled diffuser against an actual one is not applied for each air diffuser, since the focus is on large-scale air circulation induced by the diffuser in each case. The calculation mesh of each case is shown in Table 1, with each mesh having 1.7~2.2 million elements. The order of the mesh-discretized width is $O(10^{-2})$ m. These calculation cases don't treat the thermal transportation since they focus on the relation between the inlet-outlet layout and the decay process of expiratory aerosol, therefore heat sources such as human bodies are not considered.

Calculation method

The calculation conditions are shown in Table 2. In this paper, modified OpenFOAM-1.7.1 was used as the solver. OpenFOAM is an open-source CFD solver developed by Henry Weller and others. (Weller et al., 1998). In this study, LES was used. As the Sub-grid scale (SGS) model, the Standard Smagorinsky model (Smagorinsky, 1963) was adopted, and the Smagorinsky Coefficient was set as Cs=0.12. In the LES calculation, the concentration transport equation is carried out to evaluate the age of the air, and the SGS Schmidt number is Sc_{SGS}=0.5. Prior to the LES calculation, RANS employed with standard k-e model simulations were carried out to reduce the LES calculation time. After the RANS simulations, each case was processed with a 300-s calculation time for the pre-running calculation, and time-integrated for 300 s. The computational time for each case was about 10 days using the domain decomposition method and 8-way parallel processing with a PC cluster (CPU: Nehalem Xeon, 2.93 GHz, 8 cores/node).

Boundary condition

The boundary conditions are shown in Table 3, and the inlet boundary conditions for each case are shown in Fig. 2. Each case except for Case 4WC had the inflow velocity normal set to the inflow boundary plane; in Case 4WC, the inflow velocity was set at a 45-degree angle from the ceiling plane. The

fluctuation in inflow velocity for each case was generated randomly, and the standard deviation of the velocity fluctuation was set at 15 percent of the averaged inflow velocity. In each case with a wall boundary, Spalding law was applied as the near-wall velocity treatment model. To calculate the age of the air, the source term of the concentration equation was considered using 1-g/m^{3}s spatially uniform generation, with 0 g/m^3 considered as the inflow boundary.

Lagrangian calculation condition

The Lagrangian calculation conditions are shown in Table 4. As this concerns expiratory aerosol, especially coughed spit droplets, seven different diameters of particles were treated in this study (d=1, 5, 10, 30, 50, 100, 200 μm). Each particle was calculated online with LES time marching. Each particle was placed at respiratory height in a sedentary state (h=1~1.2 m, shown as the particle cloud position in Fig. 1), 50,000 particles of each diameter (350,000 particles in total) were set uniformly in the area in advance. The SGS dispersion effect for particles was not considered because the SGS effect is negligible compared with the grid-scale turbulent dispersion effect. At each wall surface, the sticking condition was applied for each diameter particle, which means such particles are removed not only from the exhaust boundary but also the wall surface.

Table 1
Calculation case

CASE	TYPE	GRID NUMBER (x × y × z)
4WC	4-Way Cassette	200 × 200 × 54 = 2,160,000 elements
BLD	Breeze-line diffuser	181 × 171 × 54 = 1,671,354 elements
SD	Square diffuser	194 × 167 × 54 = 1,749,492 elements
FD	Floor diffuser	238 × 217 × 54 = 2,788,884 elements
FSD	Floor-supply displacement	194 × 167 × 54 = 1,749,492 elements

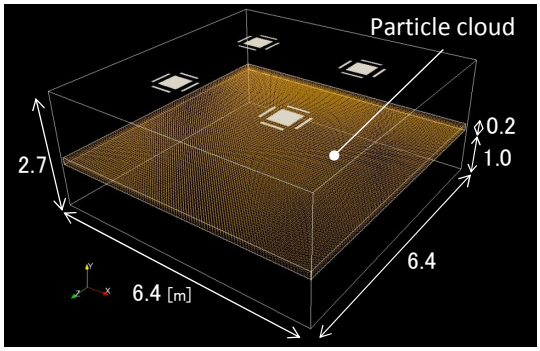

Figure 1 Calculation space and initial particle position (4-way cassette unit type)

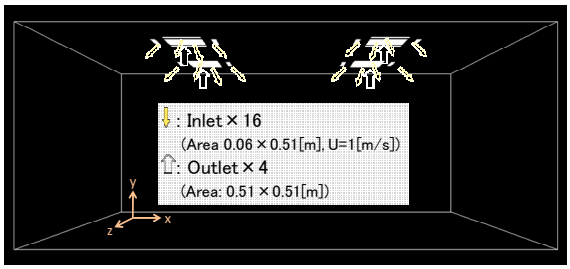

(a) 4-way cassette unit type (Case 4WC)

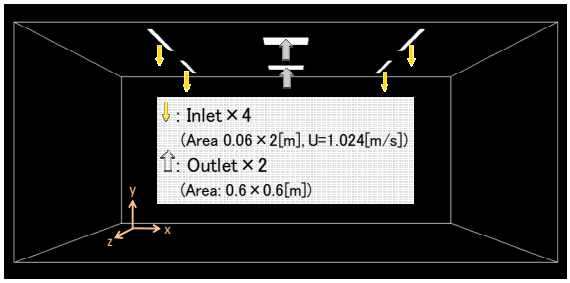

(b) Breeze-line diffuser type (Case BLD)

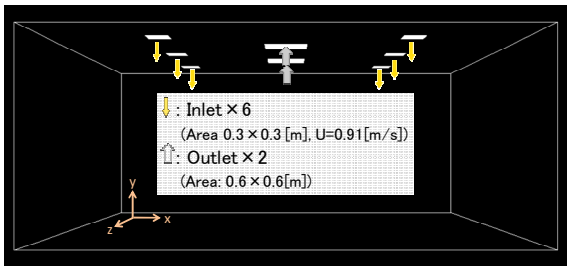

(c) Square diffuser type (Case SD)

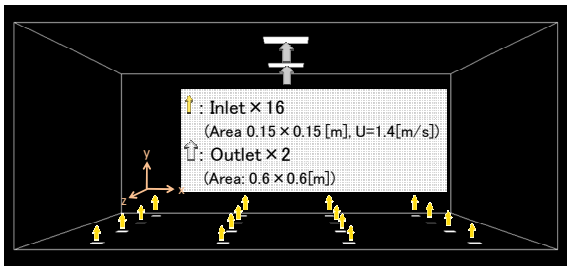

(d) Floor diffuser type (Case FD)

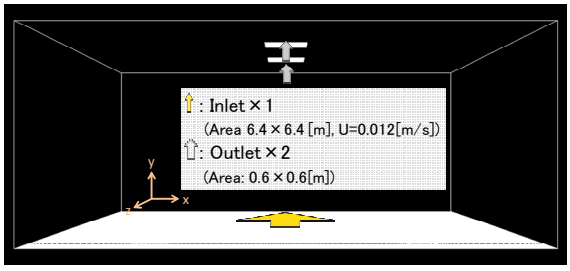

(e) Floor-supply displacement ventilation type (Case FSD)

Figure 2 Calculation space configurations for each case

Table 2
Calculation conditions

CFD solver	OpenFOAM-1.7.1
SGS model	Standard Smagorinsky (Cs=0.12)
Grid system	Finite volume method
Spatial interpolation	Convection term: 2nd order central Diffusion term: 2nd order central
Momentum-pressure coupling	PISO
Time stepping	2nd order implicit
⊿t	0.0035 s (Max Courant number is less than 0.6)

Table 3
Boundary conditions

Inflow	Momentum: refer to Fig. 2, Fluctuation: random (σ=15%) Concentration: zero
Outflow	Momentum: zero gradient Concentration: zero gradient
Wall	Momentum: Spalding's law Concentration: zero gradient

Table 4
Lagrangian calculation conditions

Material	Water (ρ=998 kg/m^3)
Diameter	D=1, 5, 10, 30, 50, 100, 200 μm
Particle momentum equation term	Drag term (Stokes' drag law), Gravity term
Dispersion model	None (Grid scale convection only)
Initial number	50,000 (of each particle diameter)
Boundary effects	Supply inlet: Reflect Exhaust outlet: Escape Solid surface: Trap

RESULTS

Scale for Ventilation Efficiency 3

The Scale for Ventilation Efficiency 3 (SVE3, Kato et al., 1992) for each case is shown in Fig. 3. The figure shows the SVE3 value for the room volume average and sedentary respiratory area (shown in Fig. 1) respectively. SVE3 is the normalized air-age value by nominal time constant. The results of RANS simulations are shown as reference. The RANS results show under-estimated values compared with LES. The room-averaged value for Case 4WC is the highest of these cases, with a value of 1.3. The other cases range between 0.8 and 1.0. The SVE3 value for Case 4WC means the room-averaged air age exceeds the nominal time constant, and this value is 60 percent higher than Cases FSD and BLD. The SVE3 contour for Case 4WC is not shown in this paper, the higher SVE3 value distribution resulting in the locally strong circulation flow of Case 4WC was pointed out from the contours. Except for Case FSD, the SVE3 for the respiratory area for each case corresponds to the room average. Case FSD shows 0.56 of the respiratory area averaged SVE3, indicating a value 40 percent lower than the room-averaged one. It seems that a one-way airflow is formed in this case because of the displacement ventilation type inlet-outlet layout.

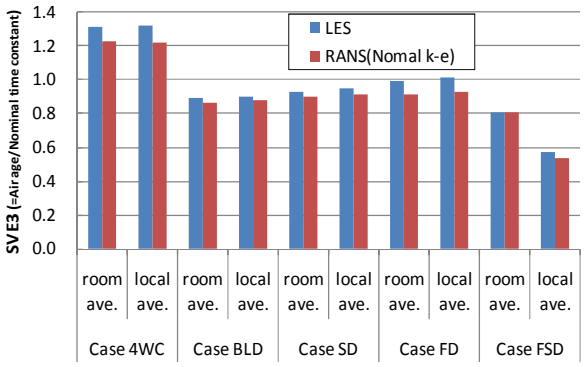

Figure 3 Comparison of SVE3

Number ratio decay of expiratory aerosol

The time history for the particle ratio remaining in the room in each case is shown in Figs. 4 and 5. Each case shows the same decay process speed as the particle diameters in d=1~50 μm, respectively. In the diameter range d=1~50 μm, Case 4WC has the slowest decay speed in these cases, followed by Case SD, then Cases BLD and FD with almost the same speed. Case FSD has the fastest decay speed of these cases. Despite having almost the same SVE3 value as Case BLD, Case FSD shows 1.4~2 times higher decay speed than the other case. Case FD exhibits the same decay process as Case BLD at d=1~5 μm. On the other hand, Case FD exhibits the same decay process as Case SD at d=10~50 μm, this tendency indicates the emerging gravitational effect and solid-surface deposition. In d=100 μm, the results of each case show different distribution compared with less than d=50 μm. In particular, the particle decay speed for Case FSD is slower than when less than d=50 μm, and shows the same decay ratio as Cases BLD and FD after 250 s. At these diameters, Case 4WC – which has an increased decay speed – corresponds to Case SD. At d=200 μm, each case demonstrates a higher decay speed. The decay speed more than doubles for each case compared with less than d=100 μm after 250 s, with very little difference between each case except for Case FSD. In Case FSD, it seems that the deposition speed balances the vertical up-flow from the floor inlet, resulting in drastic decay after 100 s and the particles were almost completely removed after 180 s.

The percentage of particles remaining after a nominal time constant in each case is shown in Fig. 6. Cases 4WC, BLD and SD categorized as ceiling inlet and

outlet types tend to exhibit a decrease in the remaining number in correspondence with the increase in particle diameter. Within these three cases, in the range d=1~50 μm, the difference between Cases 4WC and SD is 5~8 percent, while the difference between Cases BLD and SD is 5~7 percent, respectively. These results indicate that a maximum difference of approximately 30 percent occurs between the same types of ceiling inlet diffusers. In contrast to the ceiling inlet type, Case FD shows a peak in existing percentage at d=30 μm because of the opposing directions between the gravitational deposition direction and up-flow direction from the floor diffuser respectively. Because of displacement ventilation, Case FSD shows the least existing percentage in this study. However this case tends to exhibit an increase in the existing percentage at d=100 μm because of the conflict between the gravitational deposition direction and up-flow direction from the floor. Particles of d=200 μm are almost completely removed in this case, because the force of gravitational deposition exceeds the vertical up-flow preventing a recirculation flow.

The percentage of particles remaining in the respiratory area (shown in Fig. 1) in each case is shown in Fig. 7. Compared with the room-averaged figure shown in Fig. 6, the distributed value of Fig. 7 appears one seventh lower than in Fig. 6. However, the distribution trend in each case is the same Fig. 6.

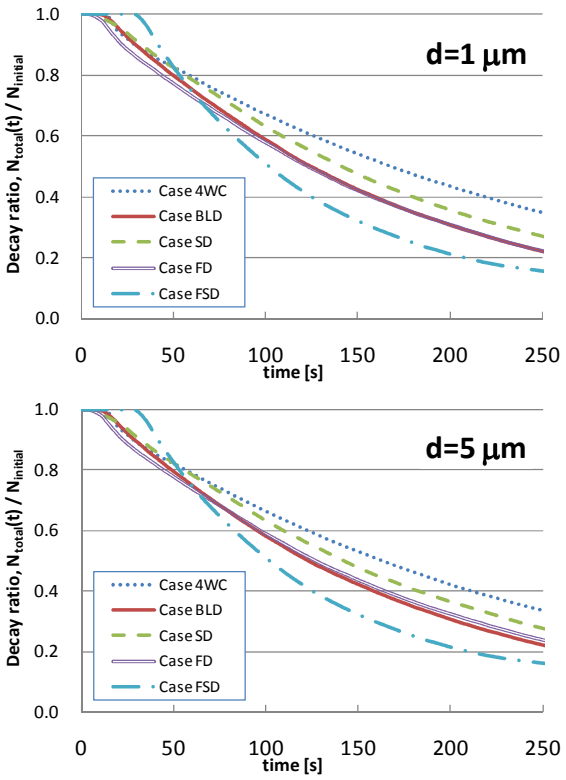

Figure 4 Decay ratio for different ventilation flow patterns (d=1 μm, 5 μm)

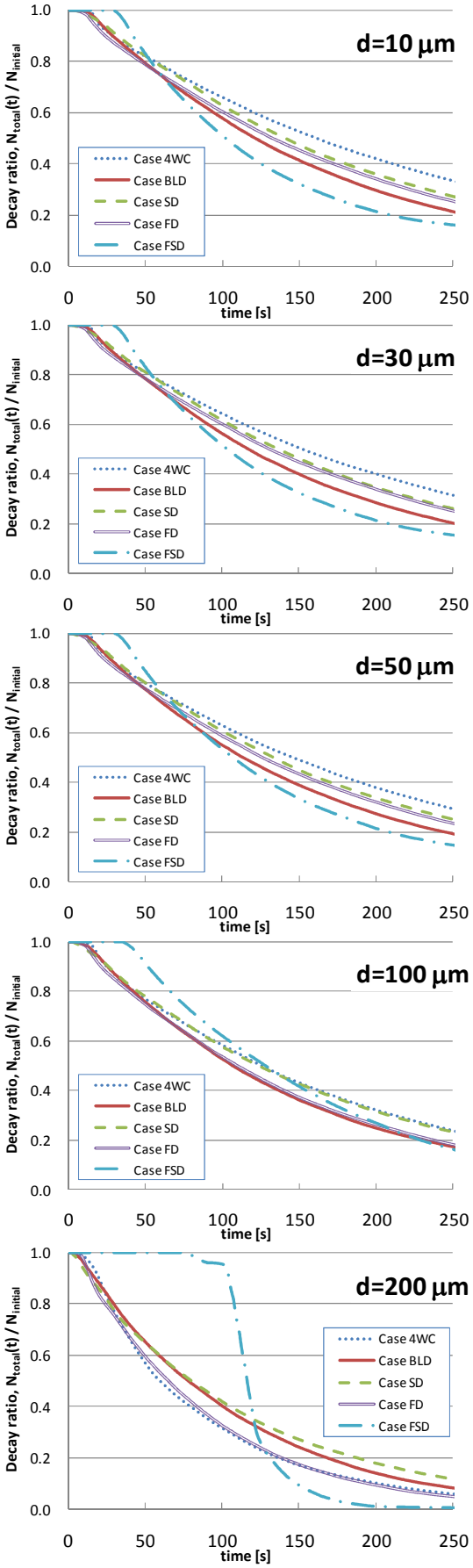

Figure 5 Decay ratio for different ventilation flow patterns (d=10 μm, 30 μm, 50 μm, 100 μm, 200 μm)

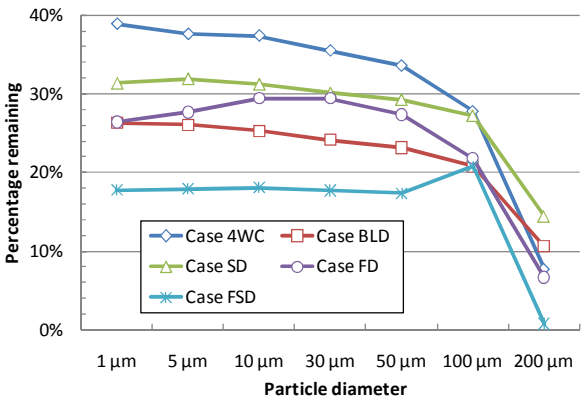

Figure 6 Percentage of particles of each diameter remaining after nominal time constant (In Room)

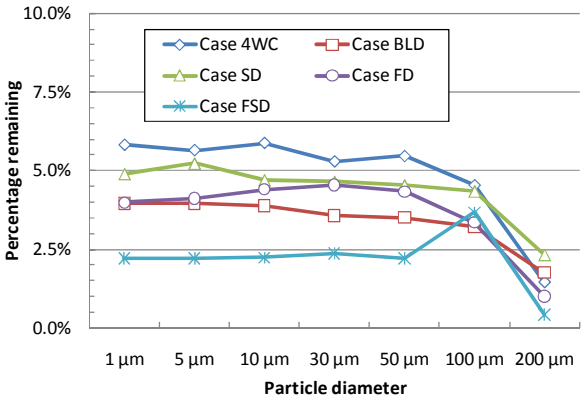

Figure 7 Percentage of particles of each diameter remaining after nominal time constant (In Respiration Area)

Percentage of particles removed

The percentage of particles removed after a nominal time constant is shown in Fig. 8 and 9. This figure also shows the removal ratio by ceiling, floor, and wall deposition and by exhaust vent. Cases 4WC, BLD, and SD, which are ceiling inlet types, show the same ratio for solid-surface deposition removal and the exhaust vent. These cases also tend to exhibit an increasing deposition ratio corresponding to the increasing particle diameter, with the ratio accounting for 20~30 percent in d=1~50 µm. On the other hand, Case FD, which is a floor diffuser type shows the same ratio of exhaust vent as the ceiling inlet type, however this case also has an increased deposition ratio. Case FSD shows the exhaust vent dominantly accounts for the removal ratio in the range d=1~100 µm, which means these particles are smoothly conveyed from the initial position to the exhaust vent without touching a solid surface. In contrast to the d=1~100 µm range, particles of d=200 µm are almost all removed by solid-surface deposition. On the other hand, another case shows that 20~30 percent of these particles are removed via the exhaust vent. The flow pattern greatly affects the removal ratio by deposition or exhaust. According to Chao et al., the mean diameters of expiratory aerosol are d=13.5 µm when coughing and d=16.0 µm when speaking (Chao et al., 2009). In terms of this study, concerning the d=10.0 µm decay characteristics, Case FSD is most efficient, followed in order by Cases BLD, FD, and SD, with Case 4WC being worst under the same ACH. Except for displacement type Case FSD, the circulation flow pattern affects the decay characteristics.

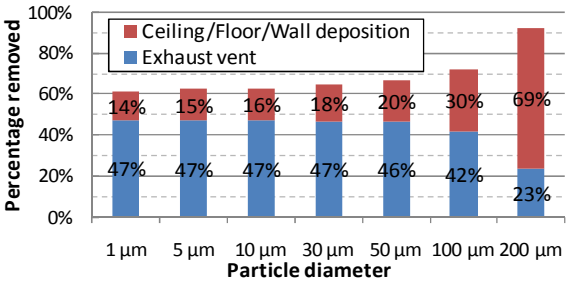

(a) Case 4WC

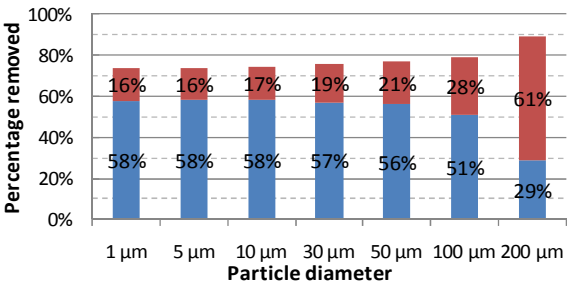

(b) Case BLD

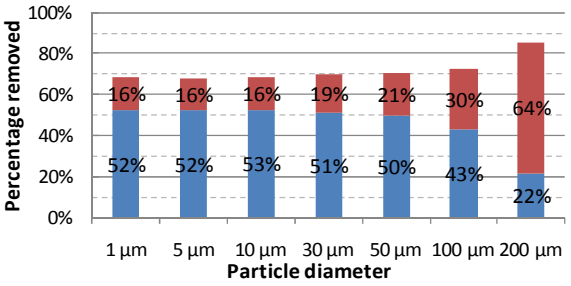

(c) Case SD

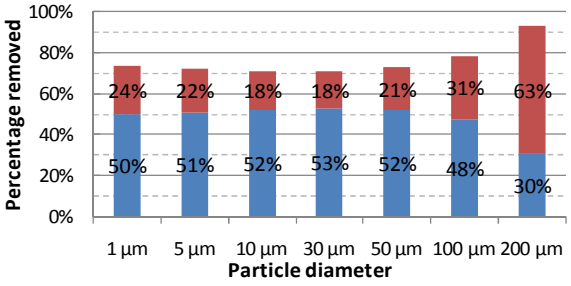

(d) Case FD

Figure 8 Percentage of particles removed by different ventilation flow patterns after nominal time constant (In Room, Case 4WC/BLD/SD/FD)

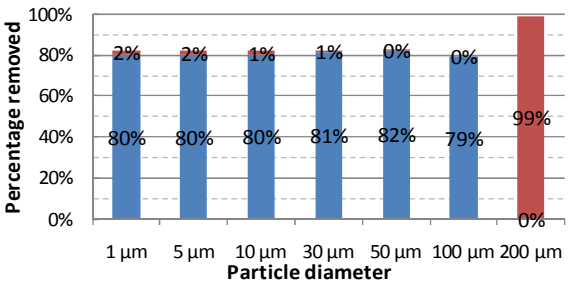

(e) Case FSD

Figure 9 Percentage of particles removed by different ventilation flow patterns after nominal time constant (In Room, Case FSD)

CONCLUSIONS

1. The decay characteristics of expiratory aerosol in indoor environments were investigated using LES coupling with Lagrangian particle tracking in terms of evaluating the ability to prevent pathogen infection in five enclosed-room cases with different diffuser-induced airflow patterns.
2. The room-averaged value for Case 4WC is the highest of these cases, with a value of 1.3. The other cases scored 0.8 to 1.0.
3. In the diameter range d=1~50 µm, Case 4WC exhibited the slowest decay followed by Case SD, with Cases BLD and FD third, both at almost the same rate. Case FSD decayed fastest among these cases.
4. Case FSD decays 1.4~2 times faster than the other comparative cases despite the SVE3 rating for this case being almost the same as Case BLD.
5. The percentage of particles remaining in the respiration area in each case was one seventh that of the room average.
6. In terms of the percentage of particles remaining after a nominal time constant, up to a 30-percent difference occurs among the same type of ceiling inlet diffusers for particles in the d=1~50 µm range.

   In terms of the decay characteristics for particles of d=10.0 µm, which is approximately the mean diameter of expiratory aerosol generated by coughing and speaking, Case FSD was most efficient, followed in order by Cases BLD, FD, and SD, while Case 4WC proved worst under the same ACH conditions.

REFERENCES

Berrouk, A. S., et al., 2010, Experimental measurements and large eddy simulation of expiratory droplet dispersion in a mechanically ventilated enclosure with thermal effects, Building and Environment, Vol.45, pp.371-379.

Bolashikov, Z. D., Melikov, A. K., 2009, Methods for Air Cleaning and Protection of Building Occupants from Airborne Pathogens, Building and Environment, Vol.44, Issue 7, pp.1378-1385.

Chao, C.Y.H., et al., 2009, Characterization of Expiration Air Jets and Droplet Size Distributions Immediately at The Mouth Opening, Journal of Aerosol Science, Vol. 40, Issue 2, pp. 122-133

Chao, C. Y. H., Wan, M. P., 2006, "A Study of the Dispersion of Expiratory Aerosols in Uni-Directional Downward and Ceiling-Return Type Airflows Using Multiphase Approach," Indoor Air, 16, 8, pp. 296–312.

Kato, S., Murakami, S. 1992. New Scales for Evaluating Ventilation Efficiency as Affected by Supply and Exhaust Openings Based on Spatial Distribution of Contaminant, International Symposium on Room Air Convection and Ventilation Effectiveness, pp.321-332

Klepeis, N. E., et al., 2001, The National Human Activity Pattern Survey (NHAPS): A Resource for Assessing Exposure to Environmental Pollutants, Journal of Exposure Analysis and Environmental Epidemiology, vol. 11, pp. 231-252.

Smagorinsky, J., 1963, General Circulation Experiments with the Primitive Equations, in the basic experiment. Monthly Weather Review, 91: pp 99-164

Sung, M., Kato, S., 2010, Method to Evaluate UV dose of Upper-room UVGI System Using the Concept of Ventilation Efficiency, Building and Environment, Vol.45, Issue 7, pp. 1626-1631.

Wan, M. P., and Chao, C. Y. H., 2007, "Transport Characteristics of Expiratory Droplets and Droplet Nuclei in Indoor Environments With Different Ventilation Airflow Patterns, Eng. Trans. ASME, 129, pp.341-353.

Weiss, R. A., McMichael, A. J., 2004, Social and Environmental Risk Factors in the Emergence of Infectious Diseases, Nat. Med., Vol.10, Issue 12, S70-S76.

Weller, H. G. et al., 1998, A tensorial approach to computational continuum mechanics using object-oriented techniques, Computers in Physics, 12-6, pp. 620–631.

Zhang, Z., et al., 2007, Evaluation of Various Turbulence Models in Predicting Airflow and Turbulence in Enclosed environments by CFD: part 2 Comparison with Experimental Data from Literature, HVAC & Research, Vol.13, pp.871-886.